Research in Astron. Astrophys. **2011** Vol. **11** No. **5**, 537–544
http://www.raa-journal.org *http://www.iop.org/journals/raa*

Research in Astronomy and Astrophysics

Submillimeter / millimeter observations of the molecular clouds associated with Tycho's supernova remnant *

Jin-Long Xu[1,2,3], Jun-Jie Wang[1,2] and Martin Miller[4]

[1] National Astronomical Observatories, Chinese Academy of Sciences, Beijing 100012, China; *xujl@bao.ac.cn*
[2] NAOC-TU Joint Center for Astrophysics, Lhasa 850000, China
[3] Graduate University of the Chinese Academy of Sciences, Beijing, 100049, China
[4] Institute of Physics, University of Cologne, Cologne 50937, Germany

Received 2010 September 16; accepted 2010 December 10

Abstract We have carried out CO $J = 2 - 1$ and CO $J = 3 - 2$ observations toward Tycho's supernova remnant (SNR) using the KOSMA 3m-telescope. From these observations, we identified three molecular clouds (MCs) around the SNR. The small cloud in the southwest was discovered for the first time. In the north and east, two MCs (Cloud A and Cloud B) adjacent in space display a bow-shaped morphology, and have broad emission lines, which provide some direct evidences of the SNR-MCs interaction. The MCs are revealed at –69∼–59 km s^{-1}, coincident with Tycho's SNR. The MCs associated with Tycho's SNR have a mass of $\sim 2.13 \times 10^3\ M_{\odot}$. Position-velocity diagrams show the two clouds to be adjacent in velocity, which means cloud-cloud collision could occur in this region. The maximum value (0.66 ± 0.10) of the integrated CO line intensity ratio ($I_{\mathrm{CO}\,J=3-2}/I_{\mathrm{CO}\,J=2-1}$) for the three MCs agrees well with the previous measurement of individual Galactic MCs, implying that the SNR shock drove into the MCs. The two MCs have a line intensity ratio gradient. The distribution of the ratio appears to indicate that the shock propagates from the southwest to the northeast.

Key words: ISM: individual objects (Tycho's supernova remnant (G120.1+1.4)) — ISM: molecules — supernova remnants

1 INTRODUCTION

When a supernova explodes near molecular clouds (MCs), shocks generated by the supernova remnant (SNR) can accelerate, compress, heat or even fragment surrounding interstellar MCs. They can also enhance abundances with respect to quiescent cloud conditions of different molecular species. Hence, the SNR-MC interaction plays a very important role in the evolution of the Interstellar Medium (Reynoso & Mangum 2000). Moreover, the molecular line observations of MCs adjacent to SNRs can shed light on the SNRs' dynamical evolution and physical properties. So far, about half of the Galactic SNRs are expected to be physically associated with MCs (Reynoso & Mangum 2001). The association is indicated by the morphological correspondence between molecular emission, the

* Supported by the National Natural Science Foundation of China.

presence of molecular line broadening within the extent of SNRs, and the presence of line emission with large high-to-low excitation line intensity ratios, as well as other factors (see Jiang et al. 2010). However, only a few cases focusing on the SNR-MC interaction have been well confirmed. Even for some SNRs interacting with the surrounding MCs, the detailed distribution of environmental molecular gas is poorly known.

Tycho's SNR is known as a young type Ia SNR located in the Perseus arm (Albinson et al. 1986), with an age of about 400 yr. The distance to Tycho's SNR is estimated to be 2.3 kpc (Kamper & van den Bergh 1978; Albinson et al. 1986; Strom 1988). The remnant has been widely studied in various wavebands. From neutral hydrogen HI observations, Schwarz et al. (1995) concluded that the distance should be 4.6±0.5 kpc; Reynoso et al. (1999) performed an HI absorption study toward the remnant, suggesting that Tycho's SNR is currently interacting with a dense HI concentration in the northeast ($V_{\rm LSR} = -51.5$ km s^{-1}), which locally slows down the expansion of the shock front. Observations in the radio continuum (Reynoso et al. 1997) and high-resolution X-ray wavebands (Hwang et al. 2002) indicated that the radio continuum and X-ray emission along the northeastern edge of Tycho's SNR is strongest. Based on the VLA observation, Dickel et al. (1991) showed that the northeastern edge of Tycho's SNR is expanding into the dense interstellar medium with a very small and decreasing velocity, and may interact with it. Lee et al. (2004) made the CO $J = 1 - 0$ line observation toward Tycho's SNR. They concluded that most of the CO $J = 1 - 0$ emission around Tycho's SNR is moving between –67 and –60 km s^{-1}, but the velocity component in the range –63.5∼–61.5 km s^{-1} appears to be in contact with Tycho's SNR along its northeast boundary. Using the CO $J = 1 - 0$ line to study the environs of Tycho's SNR, Cai et al. (2009) found that the CO $J = 1 - 0$ emission forms a semi-closed molecular shell around the SNR; emission in the velocity range –69∼–58 km s^{-1} is associated with the SNR. Because the calculated virial mass of clumps is greater than their gravitational mass, they suggested that CO molecular clumps are being violently agitated by Tycho's SNR shock.

In order to understand the evolution of the SNR interacting with MCs and investigate the detailed distribution of the molecular gas around Tycho's SNR, we have performed CO $J = 2 - 1$ and CO $J = 3-2$ observations toward Tycho's SNR. The observations cover the whole area of Tycho's SNR in these frequencies for the first time. Due to the observed molecular lines at higher frequencies, we can attain a higher angular resolution, which is critical for identifying the relatively compact core. Also, higher J transitions are relatively more sensitive to hot gas. Thus, we can understand the distribution of the molecular gas in the vicinity of Tycho's SNR with better detail.

2 OBSERVATIONS

The observations of Tycho's SNR were made in CO $J = 2 - 1$ and CO $J = 3 - 2$ lines using the 3m KOSMA sub-millimeter telescope at Gornergrat, Switzerland in January, 2004. The half-power beam widths of the telescope at observing frequencies of 230.538 GHz and 345.789 GHz, were $130''$ and $80''$, respectively. The pointing and tracking accuracy was better than $10''$. The system temperature was about 120 K. The medium and variable resolution acousto-optical spectrometers used have 1501 and 1601 channels, with a total bandwidth of 248 MHz and 544 MHz, and equivalent velocity resolution of 0.21 km s^{-1} and 0.29 km s^{-1}, respectively. The beam efficiency $B_{\rm eff}$ was 0.68 and 0.72 at 230 GHz and 345 GHz, respectively. The forward efficiency $F_{\rm eff}$ was 0.93. Line intensities were converted using the main beam scale, following the formula $T_{\rm mb} = F_{\rm eff}/B_{\rm eff} \times T_{\rm A}^{*}$.

Mapping observations were centered at RA(J2000) = $00^{\rm h}25^{\rm m}22.7^{\rm s}$, Dec(J2000) = $64°08'50.44''$ using the On-The-Fly mode; the total mapping area was $14.5' \times 15'$ with a $0.5' \times 0.5'$ grid. The observed data were reduced using the CLASS (Continuum and Line Analysis Single-Disk Software) and GREG (Grenoble Graphic) software.

The 1.4 GHz radio continuum emission data were obtained from the NRAO VLA Sky Survey (NVSS; Condon et al. 1998).

3 RESULTS

Figure 1 (Left) shows the MCs' CO $J = 2 - 1$ distribution around Tycho's SNR. The SNR appears as a complete shell on the whole and forms bright knots toward the southwest, which were detected by the 1.4 GHz continuum radio emission. Three MCs were clearly identified around Tycho's SNR. Each has been designated alphabetically: Cloud A, Cloud B, and Cloud C. In Figure 1 (Left), Clouds A–C are clearly associated with the 1.4 GHz radio continuum emission of Tycho's SNR. It appears that Clouds A and B are spatially adjacent. Here, Cloud C is identified around Tycho for the first time. Figure 1 (Right) shows the CO $J = 2 - 1$ spectra towards the peak positions of Clouds A–C, respectively. From these spectra, we can see that there are several equal-velocity components in intervals –70 $\sim$ -53 and –7$\sim$2 km s^{-1}. The velocity component in interval –7$\sim$2 km s^{-1} should belong to the foreground source (Cai et al. 2009). A double-peaked feature is observed in intervals $-70 \sim -53$ km s^{-1} for Clouds A and B, which can be fitted by Gaussians, respectively. Applying the rotation curve of Clemens (1985) together with $V_0 = 220$ km s^{-1}, where V_0 is the circular rotation speed of the Galaxy, we obtained the distances of Clouds A–C. Tycho's SNR exhibits a complete shell structure of about $8'$ in diameter. In view of the morphological correspondence of Tycho's SNR and Clouds A–C, the tangent point (the center of the SNR) in the direction to the SNR is at $\sim$4.9 kpc, which is rather close to the distance 4.6$\pm$0.5 kpc obtained from the neutral HI absorption observation (Schwarz et al. 1995). The fitted and derived parameters for Clouds A–C are summarized in Table 1. Cloud A and B have two components of velocity, as seen from the two peaks in the spectra of cloud A and B in Figure 1 (Right).

In Table 1, the clouds have broad emission lines. For Cloud A, the distance of the component showing a peak at –56.8 km s^{-1} is 4.4 kpc, which is smaller than that of Tycho's SNR ($\sim$4.9 kpc), so this velocity component can be related to foreground Galactic gas emission. Other components in intervals –70 $\sim$ –53 km s^{-1} will be analyzed below with respect to Tycho's SNR.

The present high-J transition observations enable us to map the molecular gas toward Tycho's SNR. After a careful inspection of the CO component in the range –70$\sim$–53, we find that range

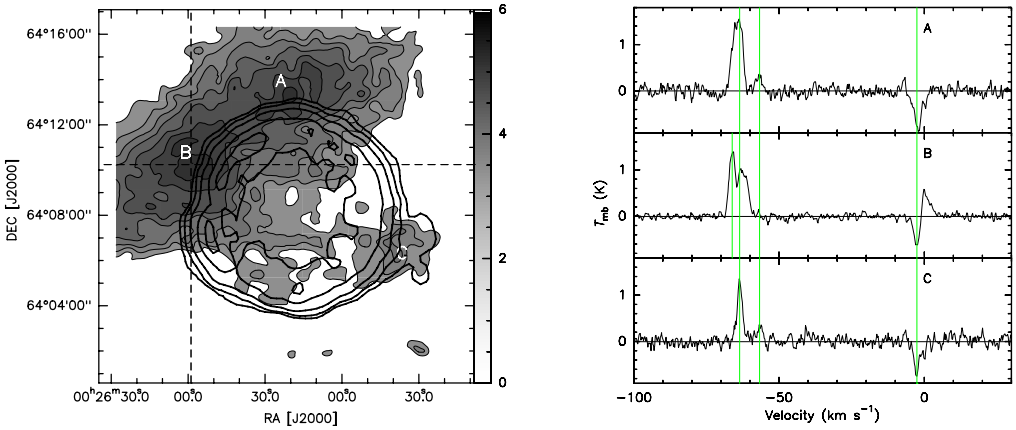

Fig. 1 *Left*: CO $J = 2 - 1$ intensity map (*gray scale*) integrated from –69 to –54 km s^{-1}, overlaid on the NVSS 1.4 GHz radio continuum emission contours (*black contours*). Gray scale levels are from 1.7 to 5.6 K km s^{-1} (1σ value is 0.15 K km s^{-1}). Two dashed lines mark the direction of the cuts in Fig. 4. *Right*: Spectra of molecular line CO $J = 2 - 1$ at the peak position of the A–C cloud clumps. Letters A, B and C indicate the different MC clumps. The vertical lines in the spectra mark the peak velocities.

Table 1 Spectral Line Parameters at the Peak Positions of the Clouds

Name	RA (h m s)	Dec (° ′ ″)	$T_{\rm mb}$ (rms) (K)	FW (rms) ($\rm km\,s^{-1}$)	$V_{\rm LSR}$ (rms) ($\rm km\,s^{-1}$)	I (rms) ($\rm K\,km\,s^{-1}$)	Distance (kpc)
Cloud A	00 25 20.7	64 13 20.44	1.6(0.2)	9.7(0.2)	–63.7(0.1)	6.7(0.2)	4.9
	00 25 20.7	64 13 20.44	0.4(0.2)	6.6(0.5)	–56.8(0.2)	1.0(0.2)	4.4
Cloud B	00 25 38.7	64 10 20.44	1.1(0.1)	9.7(0.3)	–63.5(0.1)	4.5(0.2)	4.9
	00 25 38.7	64 10 20.44	1.2(0.1)	6.3(0.1)	–66.2(0.1)	3.1(0.3)	5.0
Cloud C	00 25 02.7	64 06 20.44	1.3(0.2)	7.0(0.1)	–63.6(0.1)	3.0(0.1)	4.9

is the only channel map which can show the possible morphological and kinematical signatures of interactions between Tycho's SNR and the surrounding MCs.

Figure 2 shows the CO $J = 2 - 1$ intensity channel maps over the velocity range of $-70 \sim -53\,\rm km\,s^{-1}$ with intervals of $1\,\rm km\,s^{-1}$. The continuum radio emission is indicated as black contours.

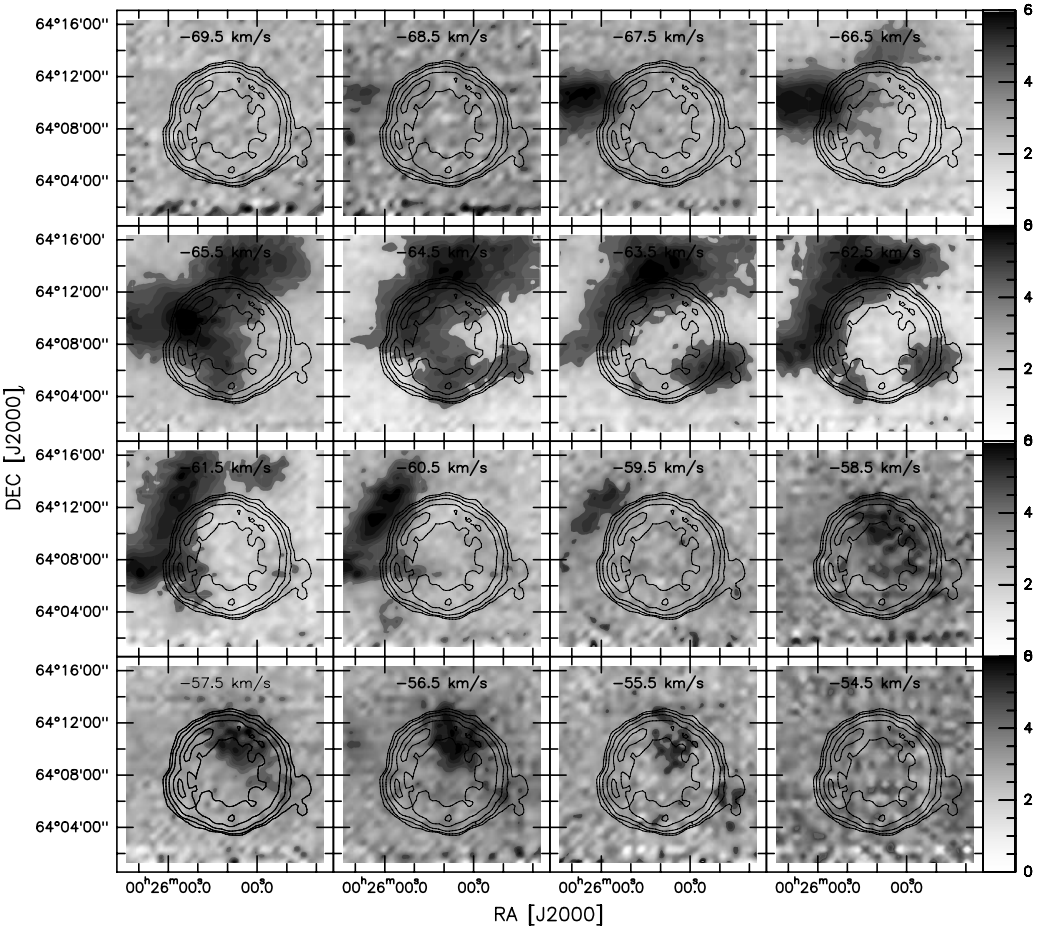

Fig. 2 CO $J = 2 - 1$ channel maps with intervals of $1\,\rm km\,s^{-1}$, overlapping the NVSS 1.4 GHz continuum radio emission. The continuum radio emission is indicated as black contours. Central velocities are indicated in each image.

There is virtually no CO $J = 2-1$ emission at $V_{\rm LSR} > -54$ km s^{-1} and $V_{\rm LSR} < -69$ km s^{-1}, and most of the emission is between –69 km s^{-1} and –59 km s^{-1}. In addition, Cloud A's position has some faint emission in intervals –59∼–54 km s^{-1}. The faint emission corresponds to a CO component peaked at –56.8 km s^{-1}, as seen from the CO $J = 2-1$ spectra of Cloud A in Figure 1 (Right), which can be related to the foreground Galactic gas emission from the above analysis. Furthermore, the Cloud A position has some strong emission in intervals –67∼–59 km s^{-1}, which can be related to a CO component peaked at –63.7 km s^{-1}. This component shows an arc of molecular gas which is strikingly coincident with the SNR along the northeast boundary. In Figure 2, there are two velocity components in the intervals –69∼–64 and –67∼–59 km s^{-1} for Cloud B, corresponding to peaks at –66.2 km s^{-1} and –63.5 km s^{-1} in the spectra (see Fig. 1), respectively. The CO $J = 2-1$ component at –69∼–64 km s^{-1} appears to be in contact with the remnant along its eastern boundary. In addition, we can clearly see that the CO $J = 2-1$ molecular gas in the southwest in the range –65∼–61 km s^{-1} corresponds to Cloud C.

The different transitions of CO trace different molecular environments. In order to obtain the integrated intensity ratio of CO $J = 3-2$ and $J = 2-1$ ($I_{{\rm CO}\,J=3-2}/I_{{\rm CO}\,J=2-1}$), we convolved the 80″ of CO $J = 3-2$ data with an effective beam size of $\sqrt{130^2 - 80^2} = 102''$ (Qin et al. 2008). The integrated intensities were calculated for the CO $J = 2-1$ line in the same velocity range as for CO $J = 3-2$. The integrated range is from –69 to –54 km s^{-1}. The rms noise level is 0.15 K km s^{-1}(1σ).

Figure 3 shows the distribution of the ratio (color scale) overlaid with the distribution of the integrated CO $J = 2-1$ line intensity (black dashed contours). The radio continuum emission is indicated as black contours. The ratio values for Clouds A–C are between 0.23 and 0.66. The rms level is 0.10 (1σ). The maximum value for the three MCs is 0.66, which is in agreement with the value measured in the Milky Way (0.55±0.08; Sanders et al. 1993), in NGC 253 (0.5±0.1 in the disk; Wall et al. 1991), and in M33 (0.69±0.15; Wilson et al. 1997). It also appears to be near the value measured in the starburst galaxy M82 (0.8±0.2; Güsten et al. 1993). In Figure 3, the high ratios (red color) are shown in the northeast part of Clouds A and B. The ratio value in this region is greater than that in the region where the cloud overlaps Tycho's SNR. The clouds have a ratio value gradient which increases from southwest to northeast, suggesting that the SNR shock is expanding into Clouds A and B, and is starting to compress the clouds.

Assuming local thermodynamical equilibrium (LTE) for the gas and an optically thick environment for the CO $J = 2-1$ line, we use the relation $N_{\rm H_2} \approx 10^4 N_{\rm CO}$ (Dickman 1978). The column density is estimated as (Garden et al. 1991)

$$N_{\rm CO} = 6.9 \times 10^{14} \frac{T_{\rm ex} + 0.92}{\exp(-11.1/{\rm T_{ex}})} \int T_{\rm mb} dv \ {\rm cm}^{-2} \, . \quad (1)$$

The excitation temperature ($T_{\rm ex}$) of the CO $J = 2-1$ line is estimated following the equation $T_{\rm ex} = 11.1/\ln[1 + 1/(T_{\rm mb}/11.1 + 0.02)]$, where $T_{\rm mb}$ is the corrected main beam temperature. Furthermore, their mass is given by $M = \mu N_{\rm H_2} S/(2.0 \times 10^{33})$, where the mean atomic weight of the gas μ is 1.36. S is the size of the core region. The physical parameters of the core are summarized in Table 2.

Table 2 Physical Parameters of the Core in LTE

Name	R (pc)	$T_{\rm ex}$ (K)	$N_{\rm CO}$ (10^{17} cm^{-2})	$N_{\rm H_2}$ (10^{21} cm^{-2})	M ($M_\odot$)
Cloud A	5.1	5.7	2.2	2.2	1151
	1.4	3.8	0.6	0.6	25
Cloud B	2.8	5.0	1.7	1.7	275
	5.0	5.1	1.1	1.1	581
Cloud C	2.1	5.3	1.1	1.1	96

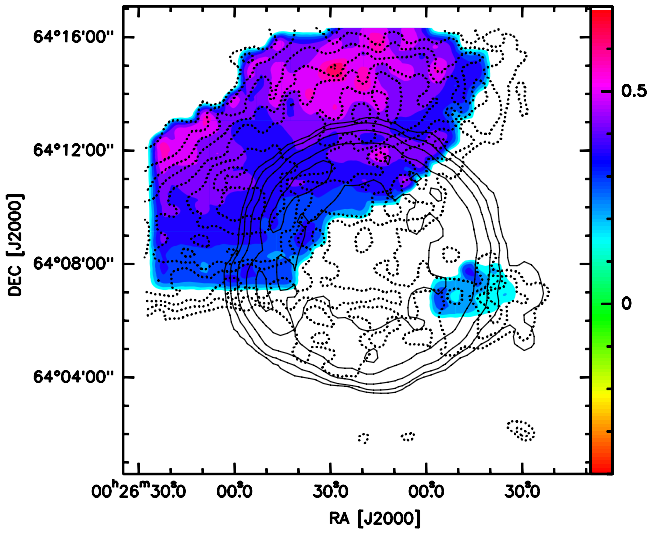

Fig. 3 CO $J = 2 - 1$ intensity map (*dashed line*) is superimposed on the line intensity ratio map (*color scale*); the line intensity ratios ($I_{\mathrm{CO}\,J=3-2}/I_{\mathrm{CO}\,J=2-1}$) range from 0.13 to 0.66 in steps of 0.06. The rms level is 0.10 (1σ). The colored bar on the right indicates the line intensity ratios scale. Black contours indicate the NVSS 1.4 GHz radio continuum emission.

4 DISCUSSION

Tycho's SNR has a complete radio shell and bright radio knots in the southwest. Among the MCs surrounding Tycho's SNR, we have seen that three clouds (Cloud A, Cloud B and Cloud C) are spatially coincident with the SNR. Broad emission lines detected in Clouds A and B and bow-shaped morphology suggest that the MCs may be interacting with the SNR. After a careful inspection of the CO component, we find that the CO component of Cloud A in the range –67∼–59 km s^{-1} (peaked at –63.7 km s^{-1}) and the CO component of Cloud B in the ranges –69∼–64 km s^{-1} (–66.2 km s^{-1}) and –67∼–59 km s^{-1} (–63.5 km s^{-1}) are clearly associated with Tycho's SNR. The position-velocity diagram across the peak of Cloud B along the north-south and the east-west directions, respectively, are constructed from the CO $J = 2 - 1$ line (see Fig. 4). In Figure 4, obviously, the velocity components of Cloud A and Cloud B are adjacent. For Cloud A, the CO component in the range –67∼–59 km s^{-1} may belong to Cloud B, because Clouds A and B are adjacent in space and velocity, and have approximately the same peak velocity in the associated spectra. We concluded that Clouds A and B may not only simply be overlapping along the line of sight, but are also colliding with each other. Furthermore, the newly found Cloud C is also clearly associated with bright knots; the bright knots may be a radio emissivity increase due to compression of the shocked material, suggesting that Cloud C appears to be swept up by the SNR shock in the southwestern area.

The maximum value of the integrated CO line intensity ratio for the three MCs is 0.66±0.10. The comparison with previously published observations reveals that the $I_{\mathrm{CO}\,J=3-2}/I_{\mathrm{CO}\,J=2-1}$ for the MCs associated with Tycho's SNR agrees well with the value measured in Milky Way (0.55±0.08; Sanders et al. 1993), in NGC 253 (0.5±0.1 in the disk; Wall et al. 1991), and in M33 (0.69±0.15; Wilson et al. 1997). It also appears to be near the value measured in the starburst galaxy M82 (0.8±0.2; Güsten et al. 1993). The high $I_{\mathrm{CO}\,J=3-2}/I_{\mathrm{CO}\,J=2-1}$ value in starburst galaxies may be due to unusual conditions in these dense and hot regions (Aalto et al. 1997), but for normal MCs, the most likely explanation is a significant contribution to the CO emission by low column density material (Wilson & Walker 1994). Moreover, the high $I_{\mathrm{CO}\,J=3-2}/I_{\mathrm{CO}\,J=2-1}$ value (3.4) in the

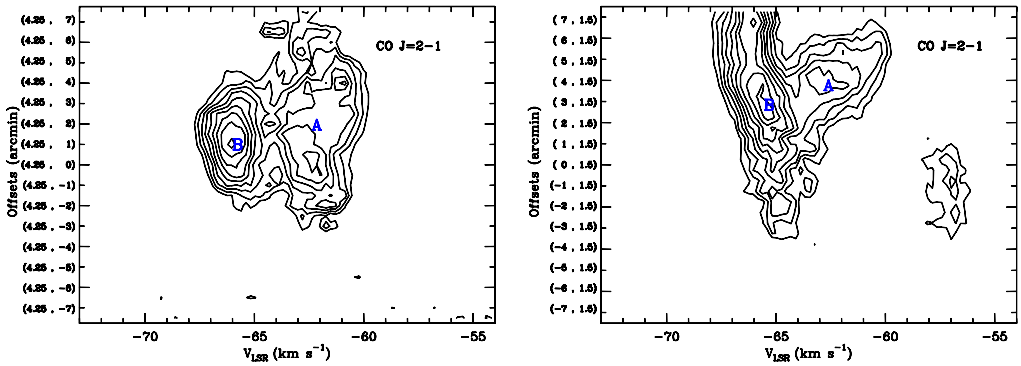

Fig. 4 P-V diagram constructed from the CO $J = 2 - 1$ transition for Cloud B. *Left panel*: Contour levels are from 0.3 K to 4.4 K in steps of 0.1 K, with a cut along the north-south direction. *Right panel*: Contour levels are the same as in the left panel, with a cut along the east-west direction.

MCs interacting with SNR IC443 (Xu et al. 2010) exceeds the previous measurement of individual Galactic MCs, implying that the SNR shock has driven into the MCs. For the MCs around Tycho's SNR, the $I_{\mathrm{CO}\,J=3-2}/I_{\mathrm{CO}\,J=2-1}$ value (0.66±0.10) may indicate that the the shock from Tycho's SNR just recently drove into the surrounding MCs. In addition, the MCs associated with HII regions have a higher ratio of $I_{\mathrm{CO}\,J=3-2}/I_{\mathrm{CO}\,J=2-1}$ and have higher gas temperature than those sources without HII regions, indicating that the high line ratio may be due to heating of the gas by the massive stars (Wilson et al. 1997). Different masers may be occurring in different astrophysical environments. The $\mathrm{H_2O}$ masers are located near the MSX sources and within the maximum line intensity ratio $I_{\mathrm{CO}\,J=3-2}/I_{\mathrm{CO}\,J=2-1}$ regions, suggesting that $\mathrm{H_2O}$ masers occur in relatively warm environments (Qin et al. 2008). Thus, we concluded that the line intensity ratios based on the optically thick CO transitions indicate that the temperature varies at different positions. The MCs associated with Tycho's SNR have a ratio value gradient that increases from southwest to northeast, which may imply that a shock has been driven into the MCs and compressed them. The MCs being compressed leads to the temperature of molecular gas increasing. Hence, the line intensity ratio $I_{\mathrm{CO}\,J=3-2}/I_{\mathrm{CO}\,J=2-1}$ will increase. We consider that a high value of $I_{\mathrm{CO}\,J=3-2}/I_{\mathrm{CO}\,J=2-1}$ is also identified as one good signature of an SNR-MC interacting system. From Table 2, the total mass of the MCs is $\sim 2.13 \times 10^3\ M_{\odot}$.

5 SUMMARY

We have presented a large-area map of MCs in the vicinity of Tycho's SNR using CO $J = 2 - 1$ and $J = 3 - 2$ lines. The complete map suggests that MCs are mainly distributed along the northern and eastern boundary of the SNR. It also reveals a new cloud (Cloud C) that appears to be swept by the SNR shock in the southwestern area. The bow-shaped morphology, the broad emission lines, as well as the integrated CO line intensity ratios ($I_{\mathrm{CO}\,J=3-2}/I_{\mathrm{CO}\,J=2-1}$) (0.66±0.10) further suggest that these MCs are interacting with Tycho's SNR. The MCs are revealed at –69∼–59 km $\mathrm{s^{-1}}$, coincident with Tycho's SNR. The MCs associated with Tycho's SNR have a mass of $\sim 2.13 \times 10^3\ M_{\odot}$. In the northern and eastern MCs, we find a line intensity ratio gradient along the southwest-northeast direction, implying that Tycho's SNR shock has driven into the MCs. We concluded that the line intensity ratios based on the optically thick CO transitions indicate the temperature varies at different positions. Both the integrated intensity maps and position-velocity diagrams show the eastern and northern clouds to be adjacent in space and velocity. Together with approximately the same peak velocity in spectra, we found that the two MCs are interacting, indicating possible cloud-cloud collision in this region.

Acknowledgements We are very grateful to the anonymous referee for his/her helpful comments and suggestions. This work was supported by the National Natural Science Foundation of China (Grant No. 10473014).

References

Aalto, S., Radford, S. J. E., Scoville, N. Z., & Sargent, A. I. 1997, ApJ, 475, L107
Albinson, J. S., Tuffs, R. J., Swinbank, E., & Gull, S. F. 1986, MNRAS, 219, 427
Cai, Z.-Y., Yang, J., & Lu, D.-R. 2009, Chin. Astro. Astrophys., 33, 393
Clemens, D. P. 1985, ApJ, 295, 422
Condon, J. J., Cotton, W. D., Greisen, E. W., Yin, Q. F., Perley, R. A., Taylor, G. B., & Broderick, J. J. 1998, AJ, 115, 1693
Dickel, J. R., van Breugel, W. J. M., & Strom, R. G. 1991, AJ, 101, 2151
Dickman, R. L. 1978, ApJS, 37, 407
Garden, R. P., Hayashi, M., Hasegawa, T., Gatley, I., & Kaifu, N. 1991, ApJ, 374, 540
Güsten, R., Serabyn, E., Kasemann, C., Schinckel, A., Schneider, G., Schulz, A., & Young, K. 1993, ApJ, 402, 537
Hwang, U., Decourchelle, A., Holt, S. S., & Petre, R. 2002, ApJ, 581, 1101
Jiang, B., Chen, Y., Wang, J., Su, Y., Zhou, X., Safi-Harb, S., & DeLaney, T. 2010, ApJ, 712, 1147
Kamper, K. W., & van den Bergh, S. 1978, ApJ, 224, 851
Lee, J.-J., Koo, B.-C., & Tatematsu, K. 2004, ApJ, 605, L113
Qin, S.-L., Wang, J.-J., Zhao, G., Miller, M., & Zhao, J.-H. 2008, A&A, 484, 361
Reynoso, E. M., Moffett, D. A., Goss, W. M., Dubner, G. M., Dickel, J. R., Reynolds, S. P., & Giacani, E. B. 1997, ApJ, 491, 816
Reynoso, E. M., Velázquez, P. F., Dubner, G. M., & Goss, W. M. 1999, AJ, 117, 1827
Reynoso, E. M., & Mangum, J. G. 2000, ApJ, 545, 874
Reynoso, E. M., & Mangum, J. G. 2001, AJ, 121, 347
Sanders, D. B., Scoville, N. Z., Tilanus, R. P. J., Wang, Z., & Zhou, S. 1993, in AIP Conf. Proc. 278, Back to the Galaxy, eds. S. S. Holt, & F. Verter (Melville, NY: AIP), 311
Schwarz, U. J., Goss, W. M., Kalberla, P. M., & Benaglia, P. 1995, A&A, 299, 193
Strom, R. G. 1988, MNRAS, 230, 331
Wall, W. F., Jaffe, D. T., Bash, F. N., & Israel, F. P. 1991, ApJ, 380, 384
Wilson, C. D., & Walker, C. E. 1994, ApJ, 432, 148
Wilson, C. D., Walker, C. E., & Thornley, M. D. 1997, ApJ, 483, 210
Xu, J.-L., Wang, J.-J., & Miller, M. 2010, arXiv:1011.3652